Respiratory dysfunctions in two rodent models of chronic epilepsy and acute seizures and their link with brainstem serotonin system

Hayet Kouchi [1,2], Michaël Ogier [3], Gabriel Dieuset [4], Anne Morales [1,2], Béatrice Georges [1,2], Jean-Louis Rouanet [5], Benoît Martin [4], Philippe Ryvlin [6], Sylvain Rheims [1,2,7*], Laurent Bezin [1,2*]

1. Lyon Neuroscience Research Center, Inserm U1028, CNRS UMR5292, Lyon 1 University, Lyon, France ;
2. Epilepsy institute, Bron, France;
3. IRBA, Institut de Recherche Biomédicale des Armées, Brétigny-sur-Orge, France;
4. Univ Rennes, CHU Rennes, Inserm, LTSI (Laboratoire de Traitement du Signal et de l'Image), UMR-1099, Rennes, France;
5. Laboratoire d'Ecologie des Hydrosystèmes Naturels et Anthropisés, U5023, Lyon 1 University, Lyon, France;
6. Department of Clinical Neurosciences, Centre Hospitalier Universitaire Vaudois, Université de Lausanne, Lausanne, Switzerland.
7. Department of Functional Neurology and Epileptology, Hospices Civils de Lyon, Lyon, France.

* co-last authors

Corresponding author:

Laurent Bezin, CRNL UMR5292 U1028, Epilepsy institute IDEE, 59 boulevard Pinel, F-69500 Bron, France; laurent.bezin@univ-lyon1.fr; tel: +33 472 138 970.

ORCID ID:
Laurent Bezin: 0000-0001-6411-4267
Gabriel Dieuset: 0000-0002-6300-7352
Hayet Kouchi: 0000-0003-1443-0645
Benoît Martin: 0000-0002-8412-1488
Sylvain Rheims: 0000-0002-4663-8515

Number of figures: 5
Number of tables: 1
Supplementary figures: 2
Supplementary table: 1

38 **Abbreviations:** 5-HT, serotonin; AGS, audiogenic seizures; EPI; CIH, chronic intermittent
39 hypoxia; EEG, electro-encephalography; epileptic; EPI/SDOC-, epileptic rat without sharp
40 decrease in oxygen consumption; EPI/SDOC+, epileptic rat with sharp decrease in oxygen
41 consumption; f_R, respiratory frequency; FRA, fatal respiratory arrest; HCVR, hypercapnia
42 ventilatory response; HIS, handling-induced seizures; HVR, hypoxia ventilatory response;
43 NFRA, non-fatal respiratory arrest; GTCS, generalized tonic-clonic seizures; NTS, nucleus
44 tractus solitarius; OSA, obstructive sleep apnea syndrome; Pilo-SE, pilocarpine-induced
45 *status epilepticus*; SE, *status epilepticus*; SERT, serotonin transporter; SSRI, selective
46 serotonin reuptake inhibitor; SUDEP, sudden unexpected death in epilepsy; T_E, expiration
47 time; T_I, inspiration time; Tph2, tryptophan hydroxylase 2; T_{tot}, total respiratory cycle
48 duration; $\dot{V}_E$, minute volume; VLM, ventrolateral medulla; $\dot{V}O_2$, oxygen consumption; V_T, tidal
49 volume

50 **Key words:** *status epilepticus*, Sprague-Dawley rat, DBA/2 mice, Metabolic rate of oxygen,
51 SUDEP.

52

Abstract

Patients with drug-resistant epilepsy can experience respiratory alterations notably during seizures. The mechanisms underlying this long-term alteration of respiratory function remain unclear. This study aimed at determining in rats whether epilepsy is associated with alterations of both the respiratory function and brainstem serotonin (5-HT) system. Epilepsy was triggered by pilocarpine-induced *status epilepticus* in rats. 30-50% of epileptic (EPI) rats exhibited sharp decrease of oxygen consumption (SDOC), low metabolic rate of oxygen and slow regular ventilation; these rats were called EPI/SDOC+ rats. These alterations were only detected in rats with chronic epilepsy, independent of behavioral seizures, persisted over the time, and were not associated with death. In these rats, 5-HT fiber density in the nucleus *tractus solitarius* was below that of control and EPI/SDOC- rats. Both EPI/SDOC+ rats and DBA/2 mice presenting with fatal respiratory arrest following an audiogenic-induced seizure, a model of sudden and expected death in epilepsy, had increased transcript levels of tryptophan hydroxylase 2 ($p<0.001$ for both strains) and 5-HT presynaptic transporter (rats: $p=0.003$; mice: $p=0.001$). Thus, our data support that 5-HT alterations are associated with chronic and acute epilepsy-related respiratory dysfunctions.

70 ## Introduction

71 Seizure-related respiratory dysfunctions in patients with epilepsy are well characterized and
72 can be observed either during focal seizures or during generalized tonic-clonic seizures
73 (GTCS) [1, 2]. In patients with drug-resistant epilepsy, oxygen desaturation <90%, as
74 measured by pulse oximetry, has thus been reported in 33% of focal seizures [3] and in up to
75 86% of GTCS [2]. In both seizure types, these transient hypoxemias result from ictal and/or
76 post-ictal central apnea [1, 4]. In addition, respiratory dysfunctions are not only limited to
77 seizure periods in some patients with epilepsy. Obstructive sleep apnea syndrome (OSA) is
78 thus prevalent in people with drug-resistant epilepsy ranging between 30-49% and markedly
79 exceeding the estimated rate in the general population [5, 6].

80 Importantly, these respiratory dysfunctions might represent a risk factor for sudden
81 unexpected death in epilepsy (SUDEP), which primarily results from post-ictal central apnea
82 [3], urging to fill the gap of knowledge regarding epilepsy-related respiratory alteration and
83 its pathological mechanisms. Post-mortem examination of the brainstem of patients who
84 died from SUDEP showed changes in the ventrolateral medulla (VLM) [7], a region containing
85 different populations of respiratory neurons including those of the pre-Bötzinger Complex, a
86 kernel generator of the inspiratory rhythm [8]. Specifically, SUDEP victims presented with an
87 alteration of brainstem serotonin (5-HT) system with notable decrease in both tryptophan
88 hydroxylase (TPH2), the rate-limiting enzyme in 5-HT synthesis, and 5-HT presynaptic
89 transporter (SERT) within medullary raphe nuclei and/or the VLM [7].

90 Similarly, brainstem 5-HT abnormalities have been reported in DBA/1 and DBA/2 mouse
91 strains, which are frequently used as a SUDEP model in preclinical studies because they can
92 exhibit a fatal respiratory arrest (FRA) after induction of an audiogenic seizure (AGS) [9-11].

93 Interestingly, FRAs are prevented when DBA/2 and DBA/1 mice are treated with fluoxetine, a
94 selective serotonin reuptake inhibitor (SSRI) before AGS induction, which is consistent with
95 the hypothesis that 5-HT system may have a strong implication in FRA following AGS [12, 13].
96 Nevertheless, animals prone to AGS-induced FRA present some limitations to completely
97 characterize respiratory dysfunction in chronic epilepsy and its potential associated 5-HT
98 abnormalities, mostly because they represent models of induced seizure(s) and do not
99 develop spontaneous recurrent seizures.

100 In this study, we used one of the most studied rat model of chronic epilepsy, following
101 pilocarpine-induced *status epilepticus* (Pilo-SE). As for a large number of patients with
102 temporal lobe epilepsy, Pilo-SE rats are notably characterized by chronic, spontaneous and
103 drug-resistant seizures [14]. In this model, while mortality is present during SE, no mortality
104 has been reported once chronic phase of epilepsy has developed. Thus, to further explore
105 the hypothesis that epilepsy-related respiratory alterations are associated with altered
106 brainstem 5-HT system, we first explored whether respiratory alterations occurred with
107 development of epilepsy, and then investigated whether they were associated with
108 brainstem 5-HT system alterations; i.e. number of 5-HT-positive cell bodies, density of 5-HT-
109 positive terminals, TPH2 and SERT mRNA levels. To help better conclude on the potential
110 involvement of 5-HT system alterations with respect to the respiratory disorders observed
111 during the chronic phase of epilepsy and independently of any risk of SUDEP-like mortality,
112 we finally compared brainstem TPH2 and SERT mRNA levels between EPI rats and DBA/2
113 mice exhibiting FRA after AGS.

114

115 ## Results

116 **Development of behavioral spontaneous recurrent seizures (SRSs) in rats after Pilo-SE**

117 The numbers of rats that did not develop Pilo-SE or died during SE are reported in the
118 Supplementary information section. SRSs were identified as detailed in the Methods section.
119 Briefly, out of the 82 rats subjected to Pilo-SE in experiments 1-3, 59 developed at least two
120 consecutive SRSs by the end of the 2nd week post-SE, and were then stated as EPI rats.

121 According to the evaluation of two experimenters, the number of recorded seizures (stages
122 3-5 of severity according to Racine's scale) per 12 hours during the daylight period was
123 about 1.1 ± 0.1 in EPI rats from weeks 3 to 8 after SE. In experiment 1, none of the Pilo-SE
124 rats had developed 2 consecutive Handling-Induced Seizures (HIS) at one-week post-SE, in
125 agreement with previous studies [15].

126 **A subset of EPI rats presented with abnormal pattern of oxygen consumption**

127 In experiment 1, metabolic rate of oxygen ($\dot{V}O_2$) of 20 EPI rats and 8 controls was recorded
128 for 24h each week from weeks 1 to 8 after SE. A thorough screening of $\dot{V}O_2$ was then made
129 for each rat.

130 ***Presence of sharp decreases in oxygen consumption (SDOCs).*** Control rats (n=8) presented
131 with slight up and down fluctuations of $\dot{V}O_2$ during both light and dark periods, as illustrated
132 in one rat (Figure 1A). For a better characterization of $\dot{V}O_2$ fluctuations within the daily
133 pattern, $\dot{V}O_2$ was averaged for each rat during the light and dark periods, separately.
134 Afterwards, the lowest value below the averaged $\dot{V}O_2$ was determined for each rat; it ranged
135 between 38% and 70% of their average $\dot{V}O_2$, independently of the circadian rhythm. This
136 pattern remained unchanged during the next 7 weeks of recordings. In rats subjected to
137 Pilo-SE, the pattern of daily $\dot{V}O_2$ was similar to that of controls during the first two weeks

post-SE, as illustrated in one Pilo-SE rat (Figure 1B). However, by the end of the 2nd week post-SE, two groups of EPI rats could be identified according to $\dot{V}O_2$ fluctuations. A subset of EPI rats presented with a large amplitude of $\dot{V}O_2$ decrease ("Sharp Decrease(s) in Oxygen Consumption"; SDOCs), defined as a decrease greater than -62%, a percentage that corresponds to the maximal decrease of $\dot{V}O_2$ in control rats. Such EPI rats were thus identified as EPI/SDOC+ rats and their lowest $\dot{V}O_2$ values ranged between 0% and 32% of the average $\dot{V}O_2$, as illustrated at 3 weeks post-SE in one rat (Figure 1C). By contrast, the remaining EPI rats (EPI/SDOC- rats) were similar to controls with regard to the lowest $\dot{V}O_2$ values, which ranged between 41% and 67% of the average $\dot{V}O_2$. Video monitoring confirmed that SDOCs were not associated with behavioral seizures, as illustrating while rat adopted a sleep-like position (Figure 2A). By contrast, behavioral seizures were associated with a long-lasting increase of the $\dot{V}O_2$, as illustrated during a stage-5 seizure (Figure 2B).

Regarding the highest $\dot{V}O_2$ values in control rats, they were ranged between 164% and 229% of the average $\dot{V}O_2$ (median=183%). The highest fluctuations within the daily $\dot{V}O_2$ pattern of EPI/SDOC+ and EPI/SDOC- rats were not statistically different from controls, and ranged between 144% and 227% of the average $\dot{V}O_2$ (median=180%). However, EPI/SDOC+ rats had greater increases of $\dot{V}O_2$ than those observed in EPI/SDOC- rats (+93 ± 5% *vs* +75 ± 4%; P=0.01).

As a good indicator of the stability of $\dot{V}O_2$ pattern, the intra-individual variation (coefficient of variation, CV) of the daily oxygen consumption pattern (CV-$\dot{V}O_2$) was calculated independently of light and dark periods. The mean CV-$\dot{V}O_2$ of the control group was estimated to be 20.8 ± 0.5% and 22 ± 0.7% for the light and the dark periods, respectively. The mean CV-$\dot{V}O_2$ of EPI/SDOC- rats was almost similar to that of controls with 19.1 ± 0.8%

161 and 22.8 ± 0.7% for the light and dark periods, respectively. However, in EPI/SDOC+ rats, it
162 was significantly higher than that measured in both control (P= 0.002 and p= 0.004 for light
163 and dark periods, respectively) and EPI/SDOC- groups (P< 0.0001 and p= 0.017 for light and
164 dark periods, respectively), reaching 27.4 ± 2.9% and 26.5 ± 1.3% for light and dark periods,
165 respectively.

166 ***Low metabolic rate of oxygen in EPI/SDOC+ rats.*** Since $\dot{V}O_2$ was measured weekly for all
167 rats for 8 weeks, it was possible to retrospectively assign each EPI rat into either the
168 EPI/SDOC+ or the EPI/SDOC- group from the first week after SE.

169 We investigated the evolution of the daily $\dot{V}O_2$ in each group. We first verified that SDOC
170 events in EPI/SDOC+ rats did not affect the average value of the daily $\dot{V}O_2$, both during the
171 light (P=0.86) and the dark (P=0.93) periods. Indeed, in order to compare between the three
172 groups of rats the daily $\dot{V}O_2$ during the 8 weeks of measurement, we preferred to use the
173 data without SDOCs in EPI/SDOC+ rats. We show in control and EPI/SDOC- rat groups that
174 the daily $\dot{V}O_2$ decreased progressively by 21.3 ± 2.4% (P=0.05) and 22.0 ± 2.2% (P=0.02),
175 respectively, between weeks 1-2 and 8 post-SE. By contrast, the decrease observed in
176 EPI/SDOC+ rats was much larger during the same period (-69.5 ± 1.1%; P=0.002), and already
177 reached -53 ± 6.0% (P=0.02) by the fifth week post-SE (Figure 3A). We also found that the
178 decrease of daily $\dot{V}O_2$ coincided with the onset of SDOCs (Figure 3B).

179 In each group, we verified that the daily $\dot{V}O_2$ did not change significantly between 5 and 8
180 weeks post-SE. Then, the daily $\dot{V}O_2$ has been averaged during that period for each group to
181 ease the comparison. We found that the daily $\dot{V}O_2$ was greatly reduced in EPI/SDOC+ rats at
182 5-8 weeks post-SE compared to both EPI/SDOC- rats and controls (-39 ± 7 % and -34 ± 7 %,
183 respectively). This decrease was observed during both the light period (EPI/SDOC+ *vs.*

184 EPI/SDOC- rats: p< 0.001; EPI/SDOC+ *vs.* control rats: P=0.002) and the dark period
185 (EPI/SDOC+ *vs.* EPI/SDOC- rats: p< 0.001; EPI/SDOC+ *vs.* control rats: P=0.002)
186 (Supplementary Figure S1A). At weeks 1-2 post-SE, no difference was observed between
187 groups during both light and dark periods (Supplementary Figure S1A).

188 In the 3 groups of rats (controls, EPI/SDOC+ and EPI/SDOC-), we evaluated the effect of
189 three factors that have been referenced as affecting $\dot{V}O_2$ [16]: time (t_0 corresponds to the
190 time of induction of SE in EPI rats), body weight and circadian rhythm. Full description of
191 these effects is detailed in the Supplementary information section.

192 ***Characterization of SDOCs.*** The number of SDOCs during the 24-hour measurement ranged
193 between 12 and 414 events (median = 44), with no difference of SDOC numbers between
194 dark and light periods. The median duration of SDOCs was 5 min (range: 20 sec to 13 min).
195 The longest SDOC event is illustrated in figure 2A; it lasted 13 min and occurred, according to
196 the video, during the daylight period while the animal was sleeping without any evidence of
197 behavioral seizure. Full description of $\dot{V}O_2$ pattern during the manifestation of seizures is
198 detailed in the Supplementary information section.

199 Body position during SDOCs was far different from freezing posture frequently observed
200 before rats had a behavioral seizure that was easily discernible by visual observation alone
201 (stages 3 to 5 on Racine's scale). It is also noteworthy that rats always exhibited a quiet state
202 during SDOC events. The proportion of EPI/SDOC+ rats increased between weeks 3 and 5
203 post-SE and then stabilized (from weeks 5 to 8 post-SE). By the end of the 5th week post-SE,
204 30% (6/20) of EPI rats exhibited SDOCs (Figure 3C).

205

206 **Ventilatory and cardiac functions in epileptic rats**

207 Experiment 2 aimed to further investigate respiratory function by evaluating ventilatory and
208 cardiac functions of EPI rats during chronic phase of epilepsy. It should be noted that we
209 could not record respiratory variables using whole-body plethysmography before the 10th
210 week post-SE because rats were not able to stay calm in the apparatus chamber, likely due
211 to enhanced reactivity to stressful situations.

212 ***EPI rats presented with a low steady respiratory pattern and enhanced ventilatory***
213 ***response to hypoxia and hypercapnia.*** Under normoxia, EPI rats (n=16) presented a slow
214 respiratory pattern with a significant decrease of minute ventilation ($\dot{V}_E$) compared to
215 controls (n=5) (-12 ± 3%, P=0.03) (Supplementary Figure S2A). The reduction of $\dot{V}_E$ in EPI rats
216 resulted from a decrease of respiratory frequency (f_R) (-12 ± 2% *vs* controls, P=0.001) while
217 tidal volume (V_T) was similar to controls (P=0.92). The decrease of f_R of EPI rats was related
218 to a simultaneous increase of inspiratory time (T_I) and expiratory time (T_E), that reached +20
219 ± 3% (P=0.01) and +10 ± 2 % (P=0.001) compared to the values measured in controls,
220 respectively. Consequently, the total respiratory cycle duration (T_{tot}) of EPI rats was
221 significantly higher than controls (+14 ± 2 % ; P=0.002) (Supplementary Figure S2A).

222 Regarding the stability of breathing pattern, the coefficient of variation of breathing, apnea
223 frequency and duration were similar between EPI and control rats (p=0.16, p=0.61 and
224 p=0.09, respectively) (Supplementary Figure S2B).

225 Compared to control rats (n=13), EPI rats (n=18) showed a greater hypoxia ventilatory
226 response (HVR) with higher $\dot{V}_E$ (+23 ± 6 % *vs* controls, P=0.007), higher f_R (+16 ± 2 % *vs*
227 controls, P<0.001) and similar V_T (P=0.06). Similarly, the hypercapnia ventilatory response
228 (HCVR) of EPI rats (n=18) was higher than controls (n=12) with greater $\dot{V}_E$ (+14 ± 4 % *vs*

229 controls, P=0.01) and greater f_R (+10 ± 3 % *vs* controls, p=0.02), while V_T remained similar to
230 that of controls (P=0.09).

231 ***Abnormal $\dot{V}O_2$ pattern is associated with pronounced decrease of ventilatory rhythm at***
232 ***rest.*** Since oxygen is strictly provided during ventilatory process, we aimed to compare
233 ventilation between EPI rats with or without abnormal $\dot{V}$O2 pattern. In experiment 2, we
234 were able to discriminate 8 EPI/SDOC+ rats, which presented with a daily $\dot{V}O_2$ lower than
235 that of both EPI/SDOC- rats (n=15, -51 ± 9%; P< 0.001) and control rats (n=16, -41 ± 11%;
236 P=0.003).

237 Under normoxia, the ventilation of EPI/SDOC- rats was significantly altered compared to
238 control rats (Table 1A), but to a lesser extent than that of EPI/SDOC+ rats. Indeed, compared
239 to control rats, EPI/SDOC- rats presented with a slight but not significant 6 ± 3% reduction of
240 $\dot{V}_E$, associated with an 8 ± 2% reduction (P=0.015) of f_R, a 13 ± 1% increase (P<0.001) of T_I
241 and a 9 ± 2% increase (P=0.025) of T_{tot} (Table 1A). Furthermore, compared to EPI/SDOC- rats,
242 EPI/SDOC+ rats presented with an additional 13 ± 3% reduction (P=0.013) of $\dot{V}_E$, that resulted
243 from an 8 ± 2% reduction (P=0.036) of f_R, a 13 ± 3% increase (P<0.001) of T_I and an 8 ± 3%
244 increase (P=0.013) of T_{tot} (Table 1A). Tidal volume (V_T), the coefficient of variation of the
245 breathing frequency, apnea frequency and duration were similar in all groups (Table 1A).
246 Under hypoxic and hypercapnic conditions, $\dot{V}_E$, V_T, and f_R was similar between EPI/SDOC+
247 (n=6) and EPI/SDOC- rats (n=12) (Table 1B).

248 ***No alteration of cardiac frequency and body-temperature in EPI rats.*** Respiratory system,
249 cardiac function and body-temperature have a tight relationship. In this experiment, we
250 showed that cardiac frequency and body-temperature of EPI/SDOC+ rats (n=2), EPI/SDOC-

251 rats (n=3) and control rats (n=3) were similar during both light and dark periods (Table 1C,
252 1D).

253 **Brainstem 5-HT system of EPI rats**

254 In experiment 3, 20 rats developed epilepsy. Among those rats, we identified 8 EPI/SDOC+
255 and 8 EPI/SDOC- rats. Eight control rats were used. Brainstem was processed for either
256 histological (n=3/8 rats in each group) or gene expression (n=5/8 rats in each group) analyses.

257 ***Alteration of the density of brainstem 5-HT immunopositive processes in EPI rats.*** We
258 determined whether metabolic and ventilatory alterations developed by EPI/SDOC+ rats
259 were associated with dysfunction of the 5-HT system in the brainstem. Therefore, we
260 focused our investigation within caudal raphe nuclei, which are known to innervate neuronal
261 groups closely implicated in the regulation of respiratory rhythm generation, such as the NTS
262 and the VLM. 5-HT-immunolabeling was detected in both processes and cell bodies. Within
263 caudal raphe nuclei (pallidus, magnus and obscurus), although we observed a downward
264 trend in epileptic rats, there was no statistical difference in the number of 5-HT-positive
265 neuronal cell bodies between the three groups of rats (control rats: 22 ± 6, EPI/SDOC-: 18 ± 4,
266 EPI/SDOC+: 13 ± 5, P=0.339). In addition, there was no difference in surface area of 5-HT
267 positive cell bodies (control rats: 383 ± 21 pixel^2, EPI/SDOC- rats: 445 ± 37 pixel^2, EPI/SDOC+
268 rats: 397 ± 54 pixel^2, P=0.383) nor in the index of 5-HT neuronal concentration (control rats:
269 109 ± 19 A.U., EPI/SDOC- rats: 125 ± 23 A.U., EPI/SDOC+ rats: 119 ± 18 A.U., P=0.864)
270 between the three rat groups. The density of 5-HT immunopositive processes within both
271 the VLM (Figure 4A) and the NTS (Figure 4B) was significantly higher in EPI/SDOC- rats
272 compared to EPI/SDOC+ rats and control rats (Figures 4A4 and 4B4). Furthermore, the
273 density of 5-HT-immunolabeled processes within the NTS was significantly lower in
274 EPI/SDOC+ rats compared to controls (Figure 4B4).

275 ***Alteration in brainstem transcript level of TPH2 and SERT in EPI/SDOC+ rats.*** TPH2
276 transcript level was significantly increased in EPI/SDOC+ compared to both EPI/SDOC- rats
277 and control rats. There was no statistical difference in transcript level of TPH2 between
278 EPI/SDOC- and control rats (Figure 5A). SERT transcript level was significantly increased in
279 EPI/SDOC+ compared to EPI/SDOC- rats, but not compared to control rats. In addition, SERT
280 transcript level did not differ statistically between control and EPI/SDOC- rats (Figure 5B).

281 **Brainstem 5-HT system of DBA/2 mice prone to AGS**

282 Previous studies demonstrated that almost 75% of DBA/2 mice developing AGS died from
283 fatal respiratory arrest (FRA) following a tonic hindlimb extension [17]. Among the remaining
284 mice, 15% developed non-fatal respiratory arrest (NFRA), meaning that they spontaneously
285 recovered from post-AGS respiratory arrest. Brainstem 5-HT system of DBA/2 mice
286 exhibiting FRA in response to AGS was shown to be altered in comparison with C57Black/6
287 mice that are resistant to AGS [10]. Thus, in experiment 4, we examined whether the
288 alterations of TPH2 and SERT gene expression that we have observed between EPI/SDOC+
289 rats and EPI/SDOC- rats could be found between FRA and NFRA DBA/2 mice. Among the
290 eleven male DBA/2 mice that underwent AGS with respiratory arrest, 64% of DBA/2 mice
291 presented with FRA (n=7) and 36% with NFRA (n=4). We found that the levels of TPH2 and
292 SERT transcripts were significantly elevated in FRA DBA/2 mice compared to NFRA DBA/2
293 mice (Figure 5A-B). It was striking that the level of TPH2 and SERT transcripts of FRA DBA/2
294 mice followed a trend that was similar to that of EPI/SDOC+ rats when both were compared
295 to their respective controls (NFRA DBA/2 mice and EPI/SDOC- rats).

296

297 ## Discussion

298 This study reports chronic alterations of respiratory system in epileptic (EPI) rats associated
299 with 5-HT dysfunctions within the brainstem.

300 **Exploration of respiratory function in epilepsy models.**

301 To date, studies in animal models of seizures, aimed at understanding respiratory
302 dysfunction in the context of epilepsy, were mostly performed during the time period
303 surrounding seizures, i.e. during ictal and post-ictal periods [17-27]. Respiratory alterations
304 have been detected in these abovementioned studies from short recording periods (2-30
305 min). In view of the respiratory disorders that can affect patients suffering from temporal
306 lobe epilepsy (ref), this work carried out on a widely used preclinical model of this type of
307 epilepsy (following status epilepticus induced by intraperitoneal administration of
308 pilocarpine, Pilo-SE) had two major objectives.

309 The first was to study respiratory function in rats with a long history of epilepsy and at a
310 distance from the period of brain remodeling that follows Pilo-SE-induced severe brain
311 damages [28]. After a 10-week period of active epilepsy (12 weeks post-SE), we showed a
312 decrease of breathing rhythm in epileptic (EPI) rats at rest. This result is different from that
313 reported in a recent study showing no alteration in resting ventilation in rats 2-4 weeks after
314 SE developed following intrahippocampal administration of pilocarpine [29]. However,
315 beyond the fact that we did not use the same strain of rats (Wistar vs. Sprague-Dawley in
316 our study) nor the same route of pilocarpine administration (intrahippocampally vs.
317 intraperitoneally in our study), we agree with the authors of the above-mentioned study
318 that the mechanisms leading to altered breathing may depend on the stage of epilepsy. In

319 their study, the assessment was rather at an early, whereas it was clearly at a later stage of
320 epilepsy in our study.

321 The second objective was to perform a long duration (24h) recording of the respiratory
322 function in order to extend investigation beyond the period surrounding seizure. Using
323 indirect respiratory thermochemistry, we achieved a 24-hour monitoring to determine the
324 amount of oxygen consumed by the whole-body. Subsequently, we provide evidence of the
325 presence of abnormal $\dot{V}O_2$ pattern in 30-50% of epileptic rats, which started with the
326 installation of epilepsy (2-3 weeks post-SE). These EPI rats (EPI/SDOC+ group) presented with
327 chronic $\dot{V}O_2$ abnormalities characterized by low daily pattern among which intermittent and
328 repetitive SDOC events were observed.

329 Until now, both preclinical and clinical studies investigated changes in the metabolic rate of
330 O_2 in epilepsy mostly at the brain level, reporting a decline in the activity of mitochondrial
331 respiratory complexes in rats subjected to Pilo-SE and in patients with TLE [30, 31]. In our
332 study, we measured the whole-body O_2 intake which is mostly related to gas exchange
333 during ventilatory process [32]. However, whole-body O_2 intake can be also affected directly
334 or indirectly by several factors including age, circadian rhythm, body-weight, body-
335 temperature, cardiac function and finally activity [16, 32-37]. None of these factors was
336 found to be associated with abnormal pattern of $\dot{V}O_2$ in our study. We then focused our
337 attention on the ventilatory variables that may explain abnormal $\dot{V}O_2$ pattern in a subset of
338 EPI rats.

339 **Respiratory system at rest in a subset EPI rats.**

340 The identification of several groups within a single disease is a common feature in human
341 epilepsy, but rarely described in preclinical studies. One study has dichotomized two groups

among rats subjected to kainic acid-induced SE according to the extent of brain damage and metabolic alterations [38]. In our study, EPI/SDOC+ subset has presented with a decrease of daily $\dot{V}O2$ and a severe decrease of $\dot{V}E$ compared to EPI/SDOC- group.

During a 20-min monitoring period at rest, decreases of both $\dot{V}E$ and $\dot{V}O_2$ have already been described as an inherent dysfunction in a genetic model of audiogenic seizure in the WAR rat strain [26]. Because of technical limitations (24-hour $\dot{V}O_2$ monitoring), we could not jointly assess $\dot{V}E$ and $\dot{V}O_2$ in our study, which prevented us from addressing the direct relationship that may exist between $\dot{V}E$ and $\dot{V}O_2$. Nevertheless, we estimated for each rat the $\dot{V}E/\dot{V}O_2$ ratio as an indicator of ventilatory efficiency; this ratio was significantly higher in EPI/SDOC+ rats compared with EPI/SDOC- (+52%, P=0.007) and healthy control rats (+35%, P=0.04), and not statistically different between these two latter rat groups.

It is difficult at this stage to interpret these results, especially in the context of epilepsy. However, high $\dot{V}E/\dot{V}O_2$ has already been described as an index of poor gas exchange during physical exercise of individual with heart failure disease [39]. Further exploration using blood oxygen measurement will be required to determine the direct relationship between $\dot{V}E$ and $\dot{V}O_2$ in epileptic rats following Pilo-SE. Another limitation of this study was the short duration of the ventilatory recording compared with the 24 hours of $\dot{V}O_2$ assessments. Significant fluctuations in $\dot{V}E$ could have been observed, similar to those seen for $\dot{V}O_2$, if the $\dot{V}E$ recordings had been longer. Further studies with devices allowing to concomitantly measure in free-moving rats both $\dot{V}E$ and $\dot{V}O_2$ over sufficiently long periods of time will be needed to establish a direct link between $\dot{V}O_2$ and $\dot{V}E$ profiles and specifically during SDOC events.

Indeed, these events could represent a disruption of O_2 uptake balance. But, to our knowledge, events similar to SDOCs have not yet been described and we can only interpret

365 them in the light of what we know about a dyspneic situation. A first explanation for SDOCs
366 could be the presence of ventilatory pauses; however, they would have to be extremely
367 numerous and of long duration to induce such a collapse of $\dot{V}O_2$. A second explanation could
368 be a combination of several factors; for example, the absence of gasping, especially in
369 hypoxic conditions, could lead to poor tissue oxygenation [40]. In EPI/SDOC+ rats, the $\dot{V}E$
370 signal recording was too short in duration to determine whether the absence of gasping
371 could be part of the ventilatory dysregulation.

372 **Ventilatory regulation in EPI rats.**

373 We observed an increased hypoxia ventilatory response (HVR) in EPI rats, in contrast to
374 some studies that report no alteration in HVR in Pilo-SE rats [29, 41]. In addition, EPI/SDOC+
375 and EPI/SDOC- rats exhibited a sustained hypercapnia ventilatory response (HCVR) whereas
376 previous studies have reported a diminished response in Pilo-SE-induced epilepsy, rapid
377 amygdala kindling, and WAR rat models [26, 29, 42]. It is very difficult to compare our data
378 with those in the literature, due to the fact that there are differences in models, timing of
379 respiratory recordings, and severity of exposure to hypoxia and hypercapnia between our
380 study and all others. Given that low HVR and HCVR are generally indicative of alterations in
381 peripheral or central respiratory components, their maintenance in our study may indicate
382 that if alterations occurred in the early phases, then they were compensated for or repaired
383 in the late stages of epilepsy at which we performed our investigations.

384 **Brainstem 5-HT alterations**.

385 5-HT is mostly described as an excitatory drive toward respiratory network and subsequently
386 the motor output [43]. Dysregulation of brainstem neuronal groups involved in the control
387 of breathing, particularly those of the 5-HT system, has been found in patients with drug-

388 resistant epilepsy and has been associated with an increased risk of SUDEP [7]. We found
389 that brainstem 5-HT innervation was impaired in EPI rats compared to control rats, with
390 notable differences between EPI/SDOC+ and EPI/SDOC- rats. Indeed, EPI rats presented with
391 an opposite 5-HT innervation pattern within the NTS. Since the impairment of respiratory
392 function in the EPI/SDOC- rats seem to be moderate by opposition to EPI/SDOC+ rats, it is
393 conceivable that, in these rats, the increase of 5-HT innervation in both the NTS and VLM
394 may be part of protecting mechanisms of respiratory function. Such profile of 5-HT
395 innervation was lacking in EPI/SDOC+ rats, but these rats presented with an increase of
396 brainstem levels of both TPH2 and SERT transcripts. Such mechanisms in EPI/SDOC+ rats
397 might support an increased concentration of 5-HT in neuron terminals by increasing 5-HT
398 synthesis and re-uptake of intact 5-HT molecules, respectively, and thus may represent
399 adaptive mechanisms to compensate, although not sufficiently, for the decreased brainstem
400 5-HT innervation. This conclusion is supported by results reported in conditional knock-out
401 Lmx1b mice and WAR rats, which, as for EPI/SDOC+ rats, present similar respiratory
402 alterations at rest and concomitant decrease of 5-HT drive [26, 43]. We also believe
403 according to the difference of 5-HT innervation between VLM and NTS of the same
404 EPI/SDOC+ rats that the decreasing of 5-HT could be structure specific and could be present
405 in other primary regions of respiratory regulations.

406 We also compared brainstem 5-HT system of DBA/2 mice with FRA to their closest controls,
407 DBA/2 mice with NFRA, contrasting with previous studies that compared DBA/2 mice with
408 FRA to C57BL/6 mice resistant to AGS [10]. We found an increased level of mRNA coding for
409 TPH2 and SERT in DBA/2 mice with FRA. This 5-HT profile in DBA/2 mice with FRA is
410 intriguingly similar to that of EPI/SDOC+ rats. Altered 5-HT system is thus likely involved in
411 respiratory dysfunctions in both acute and chronic seizure models.

412 In conclusion, Pilo-SE rat model, which shows both chronic respiratory alterations and
413 spontaneous seizures, could be a relevant model to further explore neurobiological
414 mechanisms underlying chronic alteration of respiratory regulation in epilepsy. Identifying
415 the mechanisms that protect EPI/SDOC+ rats from mortality might also be an interesting
416 approach to pave the way for new therapeutic strategies to prevent SUDEP.

417 Methods

418 All animal procedures were in compliance with the guidelines of the European Union
419 regulating animal experimentation (directive 2010-63), taken in the French law (decree
420 2013-118), and have been approved by the ethical committee of the Claude Bernard Lyon 1
421 University (protocol # BH-2008-11).

422 Animals

423 Five week-old male Sprague–Dawley rats (Envigo, The Netherlands) were delivered to the
424 animal facility of the Lyon 1 University (Villeurbanne, France) and housed in groups of 5 in
425 transparent polycarbonate cages. Male DBA/2 mice of breeding colony of the LTSI laboratory
426 were housed in groups of five. Rats and mice were maintained under a controlled 12-h/12-h
427 light–dark cycle, in a temperature-controlled room (24-26 °C and 21-23 °C for rats and mice,
428 respectively), with free access to food and water.

429 Experimental design

430 Full description of methods have been described in details elsewhere [11, 28, 44-46]. Rats
431 subjected to Pilo-SE are daily observed to detect spontaneous seizures until animals had
432 developed epilepsy (EPI rats). Respiratory thermochemistry set-up was used to measure

433 oxygen consumption ($\dot{V}O_2$) during 24 consecutive hours (daily $\dot{V}O_2$) for each rat. Animals of
434 this study were subjected to one of following experiments:

435 ***Experiment 1.*** To establish the time course of respiratory alterations occurring among Pilo-
436 SE rats, 4 series of 10 rats were used in this experiment. In each series, Pilo-SE was induced
437 in 8 rats and 2 rats were used as controls. Daily $\dot{V}O_2$ of each rat was measured once a week
438 from the 1st to the 8th week post-SE.

439 ***Experiment 2.*** To further investigate cardio-respiratory functions in EPI rats during the
440 chronic phase of epilepsy, Pilo-SE was triggered in 30 rats and 16 rats were used as controls.
441 At the chronic period of epilepsy (12 weeks post-SE), the resting ventilation (normoxia, 21%
442 O_2) was measured using whole-body plethysmography. Between 13-14 weeks post-SE, a
443 subset of EPI and control rats were used to evaluate ventilatory responses to hypoxia (HVR,
444 FiO_2= 9%) and to hypercapnia (HCVR, $FiCO_2$= 5%), while others underwent surgery
445 implantation of telemetric device to evaluate cardiac frequency and body temperature at 15
446 weeks post-SE. As $\dot{V}O_2$ and ventilation are intermingled processes, to visualize global state of
447 respiratory system in EPI rats, we had in-depth our data exploitation by characterizing
448 ventilatory pattern according to $\dot{V}O_2$ pattern. To note, daily $\dot{V}O_2$ of EPI and control rats was
449 measured short before plethysmography at 7-9 weeks post-SE.

450 ***Experiment 3.*** To determine whether integrity of the 5-HT system is altered in the brainstem
451 of EPI rats presenting with respiratory alterations, Pilo-SE was induced in 20 rats and 8 rats
452 were used as controls. Daily $\dot{V}O_2$ was evaluated between the 6th and the 8th week post-SE.
453 Subsequently, animals were transcardially perfused and their brains were collected and
454 processed either for histological procedures (5-HT immunodetection; n=3 in each group) or
455 for gene expression analyses (SERT and TPH2 mRNA; n=5 in each group).

456 ***Experiment 4.*** To determine whether integrity of the 5-HT system is compromised in the
457 brainstem of DBA/2 mice presenting with FRA, 11 DBA/2 mice underwent AGS followed by
458 respiratory arrest. DBA/2 mouse brains were removed right after AGS for both FRA and non-
459 fatal respiratory arrest (NFRA) DBA/2 mice. Mice with FRA were resuscitated and as for
460 NFRA mice were injected with a lethal dose of pentobarbital and perfused with NaCl.
461 Brainstem SERT and TPH2 gene expressions were measured and then compared between
462 mice with either FRA or NFRA.

463 ***In vivo* procedures**

464 ***Pilocarpine-induced SE.*** Epilepsy was triggered following Pilo-SE in 180-200 g male rats at
465 the age of 7 weeks, as previously described [28, 45]. Scopolamine methylnitrate (1 $mg \times kg^{-1}$,
466 s.c.; S-2250, Sigma-Aldrich) was administered 30 min prior to pilocarpine hydrochloride (350
467 $mg \times kg^{-1}$, i.p.; P-6503, Sigma-Aldrich). After an initial period of immobility, the onset of SE
468 was characterized by repetitive tonic-clonic activity of the trunk and the limbs, occurring
469 after repeated rearing with forelimb clonus and falling. Because SE event is a life-threating
470 condition in rats, there is a need to stop it after 2 hours by a single injection of diazepam
471 (Valium®, 10 $mg \times kg^{-1}$, i.p.; Roche). Rats were then hydrated with 2 mL of saline solution
472 (0.9% NaCl; s.c.) and transferred to individual cages. After a one-week recovery period, all
473 rats (control and treated rats) were housed in groups of 5 to avoid any stress that may result
474 from social isolation.

475 ***Animal care after Pilo-SE.*** Control and treated rats were weighted daily during the first two
476 weeks following Pilo-SE, and then every week until termination of the experiment. Daily
477 abdominal massage was performed twice a day during the first week to activate intestinal
478 motility, which is disrupted following Pilo-SE.

479 ***Detection of spontaneous recurrent seizures after Pilo-SE.*** To maintain as low as possible
480 the level of anxiety in rats subjected to Pilo-SE, electro-encephalographic recordings (EEG)
481 were not performed to detect the onset of epilepsy in our experiments. Indeed,
482 conventional EEG set-up requires that rats are housed individually in a restrictive
483 environment, which is known to enhance stress and anxiety and worsens epilepsy
484 phenotype in Pilo-SE models [47]. In addition, as mentioned below in the "whole-body
485 plethysmography" section, it is difficult to perform ventilatory recordings in animals with
486 high anxiety level.

487 It is now clearly established that rats of the Sprague-Dawley strain from the Janvier
488 Laboratories develop spontaneous recurrent seizures between 10 and 36 days after
489 induction of Pilo-SE at 42 days of age [48, 49]. Because we were using Sprague-Dawley rats
490 from Envigo Laboratories, we had to monitor the time of onset of spontaneous recurrent
491 seizures (SRSs) in our experiments. To determine whether rats were in the chronic phase of
492 epilepsy, they were manipulated daily between 09:00 and 11:00 a.m. to define the onset of
493 handling-induced seizures (HIS), which was induced by restraining rats at the level of the
494 chest with gentle pressure for 10 seconds [48]. HIS were used in our study to help
495 experimenters to define the time to start detecting the first behavioural spontaneous
496 recurrent seizures (SRSs). Thus, upon detection of 2 HIS, rats were observed by
497 experimenters for 5 consecutive hours (between 01:00 and 06:00 p.m.) over the following
498 days to detect the presence or absence of behavioural SRSs. Following Pilo-SE, rats are
499 considered epileptic once they developed at least two SRSs during the periods of the daily
500 observations. The severity of these seizures was scored from 3 to 5 on the Racine's scale [50].
501 Seizure severity of less than 3 was difficult to detect visually in this study, which was
502 conducted without daily video monitoring. Stage 3 corresponds to forelimb clonus, stage 4

503 to bilateral forelimb clonus with rearing, and stage 5 to rearing and falling or to tonic-clonic
504 seizures.

505 During the 24 hour-$\dot{V}O2$ recordings, rats were video-monitored for 12h during the light
506 period, making it possible to evaluate the number of seizures and their severity per session.

507 **Evaluation of respiratory and cardiac functions**

508 ***Open respiratory thermochemistry.*** To detect respiratory alterations in epileptic rats, we
509 used respiratory thermochemistry as an alternative approach to plethysmography, allowing
510 respiratory function to be recorded for a long period of time on fed, unrestrained and
511 unanesthetized animal. Respiratory thermochemistry mostly reflects gas exchanges and
512 allows more specifically the measurement of the oxygen consumption ($\dot{V}O_2$) with no bias
513 effect from animal's body movements on the accuracy of respiratory acquisition.

514 Oxygen consumption ($\dot{V}O_2$) was measured with sample rate of 3 acquisitions per minute,
515 under standard conditions (variation in temperature = 0°C; Ambient pressure = 760 mm Hg;
516 dry air) using an open respiratory thermochemistry system, as previously described [51]. $\dot{V}O_2$
517 was continuously recorded during 24 consecutive hours on the same thermochemistry
518 system; therefore, only one rat could be recorded each day in our experimental setting.
519 Briefly, rats were placed individually in a thermostatic recording chamber (12 L) with steady
520 airflow (4 L × min^{-1}), under a controlled 12-h/12-h light–dark cycle (light from 06:00 a.m. to
521 06:00 p.m.), and were allowed free access to food and water. Ambient temperature inside
522 the thermostatic chamber was monitored with copper-constantan thermocouples and was
523 maintained at 24-26 °C using a thermostatic container. Airflow rate was measured using a
524 Platon volumeter and converted to standard STPD (standard temperature and pressure, dry)

525 values. Fractional O_2 concentration was measured using a Servomex 1100 paramagnetic gas
526 analyzer (Taylor Instrument Analytics ltd, Sussex, UK) and $\dot{V}O_2$ was calculated. The O_2
527 analyzer was calibrated daily with pure nitrogen gas (0% O_2) and room air (20.93% O_2). Rats
528 were weighted before and after recording then $\dot{V}O_2$ values were normalized to the average
529 body weight (calculated from the weight measured before and after each recording session).
530 Rats were video-monitored during the daylight period.

531 ***Whole-body plethysmography.*** Plethysmographic chamber allows collecting ventilatory
532 variables from acquired breathing pattern signal. Ventilatory function was evaluated
533 between 09:00 a.m. and 04:00 p.m. in unrestrained, unanesthetized rats under BTPS (body
534 temperature and pressure, saturated) conditions using whole-body plethysmography
535 (EMKA; technology). Calibration of the system was performed before each recording session
536 by injecting a 1 mL air pulse inside the recording chamber. Briefly, each rat was individually
537 placed in the recording chamber (600 mL) that is connected to a constant bias flow supply
538 providing continuous inflow of fresh air (2.5 L × min^{-1}). Minute volume ($\dot{V}_E$; mL × min^{-1}) was
539 calculated as the product of tidal volume (V_T; mL) and respiratory frequency (f_R; breath x
540 min^{-1}). Total respiratory cycle duration (T_{tot}) was calculated as the sum of the inspiratory
541 time (T_I; msec) and expiratory time (T_E; msec). We also calculated for each animal the
542 coefficient of variation of the respiratory frequency, which is an index of the variability of
543 the respiratory pattern [52] and the frequency of spontaneous apnea, which is defined as a
544 cessation of breathing lasting more than two respiratory cycles (>2 x T_{tot}). Apnea number
545 and duration were calculated. Apnea frequency was normalized to recording duration and
546 expressed per min of breathing. Recordings were started after a 40-minute habituation
547 period. Then, resting ventilation was monitored during 20 minutes under normoxic condition
548 (21% O_2). After recordings, rats were brought back to their home cage.

549 Ventilatory responses to hypoxia (FiO_2= 9%) and to hypercapnia ($FiCO_2$= 5%) were evaluated
550 during two distinct recording sessions, which were performed a week apart from each other.
551 After a 40-minute habituation period, plethysmographic recordings under basal condition
552 (normoxia) were started 10 minutes before gas variations. Ventilatory responses to a 10-
553 minute exposure to hypoxia or hypercapnia were subsequently evaluated. All
554 plethysmography recordings were made between 09:00 a.m. and 04:00 p.m.; because,
555 beyond 04:00 p.m., EPI rats were more stressed in the plethysmography chamber, requiring
556 longer time to reach a quiet state in this novel and restricted environment. At the end of
557 each recording session, rats were brought back to their home cage. Repeated measurements
558 are randomly performed for each rat.

559 ***Abdominal implantation of telemetry transmitters to evaluate cardiac function and body-***
560 ***temperature.*** Rats were anesthetized with a mix of ketamine and xylazine (75 mg × kg^{-1} and
561 25 mg × kg^{-1}, respectively; i.p.). A midline abdominal incision was made and a sterile
562 telemetry transmitter (Data Sciences International, France) was placed inside the abdominal
563 cavity. A pair of biocompatible wire electrodes originating from the transmitter were
564 tunnelled subcutaneously and implanted to the left intercostal muscles and between the
565 right shoulder blades. The transmitter was attached to the abdominal wall during wound
566 closure with absorbable sutures. After surgery, animals received an intramuscular injection
567 of penicillin (15,000 units) once a day for 3 consecutive days and were then returned to their
568 home cage. Rats were monitored daily to control general health state. Two weeks after
569 surgery, telemetry transmitters were magnetically activated and freely moving animals were
570 placed in individual cages placed under platform-receiver units. Variation in cardiac
571 frequency and body-temperature were recorded during 24 consecutive hours.

572 **Induction of audiogenic seizures in DBA/2 mice**

573 AGS were induced as previously described [11, 17], with slight modifications. Briefly, at age
574 of 23 days, mice were individually placed in a plastic cylinder (40 cm diameter, 20 cm height)
575 and exposed to a broadband acoustic stimulus (intensity of 110 dB SPL with a peak
576 frequency at 12 kHz) generated by a mechanical sonicator (Deltasonic model Delta 920). The
577 stimulus was given for a maximum duration of 60 seconds or until the mouse exhibited AGS,
578 characterized by an initial wild running and ending by a tonic hindlimb extension. All mice
579 exhibited a tonic hindlimb extension leading to a respiratory arrest identified by pinnae
580 relaxation and a complete cessation of chest movements. Respiratory arrest was followed by
581 spontaneous recovery of the respiratory function within 5 seconds in mice identified as
582 NFRA, or was followed by death for the other mice (FRA). Mouse brain was systematically
583 removed within 2-3 min after acoustic stimulus was triggered.

584 ***Ex vivo* procedures**

585 DBA/2 mice and rats were injected with a lethal dose of pentobarbital (250 mg × kg^{-1}; i.p.)
586 before being sacrificed. For gene expression analyses, animals were transcardially perfused
587 (30 mL x min^{-1}) for 2 min with ice-cold saline and their brain was rapidly removed. Then, the
588 brainstem region was isolated, frozen in liquid nitrogen and stored at -80°C. For
589 immunohistochemistry procedure, animals were transcardially perfused (30 mL x min^{-1}) for 2
590 min with ice-cold saline and then for 10 min with ice-cold 4% paraformaldehyde in 0.2 M
591 phosphate buffer (30 mL x min^{-1}). After cryoprotection in a 25% sucrose solution, brains
592 were frozen at -40°C in isopentane and stored at -80°C.

593 ***5-HT immunohistochemistry.*** Coronal sections (40 µm thick) were cryostat-cut throughout
594 the medulla oblongata and were processed free-floating for 5-HT immunostaining. Using the

595 rat brain atlas, sections from each experimental group were selected at interaural
596 coordinates -2.60 mm, and were all processed together for 5-HT immunofluorescent labeling.
597 Selected sections were rinsed in 0.1M Phosphate Buffered Saline (PBS) and incubated in PBS
598 containing 0.3% Triton X-100 and 3% normal donkey serum. Then, sections were incubated
599 with a rabbit polyclonal antibody against 5-HT (Sigma; S5545; final dilution = 1:3,000). After
600 few washes, sections were incubated with an AlexaFluor-488 conjugated donkey anti-rabbit
601 antibody (Molecular Probes; A-21206; final dilution = 1:1,000). At the end of the
602 immunostaining protocol, sections were mounted onto SuperFrost®Plus slides and cover
603 slipped using Vectashield mounting medium (H-1500, Vector).

604 ***Semi-quantification of brainstem 5-HT immunostaining.*** Images (1152 x 1024 pixels) were
605 captured with a HLX PL APO x63/0.70 objective and with the same conditions of
606 photomultiplier gain, offset and pinhole aperture using a TCS SP2 confocal microscopy
607 system (Leica), allowing the comparison of fluorescence intensity between sections. Image
608 analysis was conducted on an average of 8 z-compressed images stacks (each image = 4 µm
609 depth), which include the whole region of interest. Using the image J software (NIH), we first
610 measured the average grey value within each 5-HT-positive neuronal cell body of caudal
611 raphe nuclei (pallidus, magnus and obscurus), as an index of 5-HT neuronal concentration
612 (A.U.). Using the same software, we also measured the density of 5-HT-immunopositive
613 processes within the surface area of the NTS and the VLM, expressed as 5-HT-positive pixel/
614 pixel^2.

615 ***Quantification of transcript level variation by RT-qPCR.*** Total RNA was extracted from
616 brainstem samples using Tri-reagent LS (Molecular Research Center, Inc.). Contaminant
617 genomic DNA was subsequently removed from the samples by treatment with Turbo DNA-

618 *free*™ kit (Ambion). The messenger RNAs (mRNAs) contained in 1 µg of purified RNA extracts
619 were reverse-transcribed using the reverse transcriptase RNase H minus (Promega) and
620 oligo-d(T)15. To normalize the RT step, a synthetic external and non-homologous poly(A)
621 standard RNA (SmRNA; Morales and Bezin, patent WO2004.092414) was added to the RT
622 reaction mix (150,000 copies in each experimental sample), as previously described [28, 44-
623 46]. PCR amplification of selected cDNAs, i.e. those complementary to the mRNA encoding
624 rate-limiting enzyme of brainstem 5-HT synthesis (tryptophan hydroxylase: TPH2) and the 5-
625 HT transporter (SERT), were performed using the Rotor-Gene Q system (Qiagen) and the
626 QuantiTect SYBR Green PCR Kit (Qiagen). Sequences of the different primer pairs used for
627 PCR amplification of mouse and rat TPH2 and SERT cDNAs are listed in Supplementary Table
628 S1.

629 **Statistical analysis**

630 The data for each experimental group were pooled and expressed as the mean ± SEM in the
631 text and figures, unless otherwise specified. All statistics were performed using Sigma plot
632 software 3.5 (Systat Software Inc., Point Richmond, California, USA). A Kolmogorov-Smirnov
633 test was used to test if the data follows a normal distribution, then paired or unpaired t-test
634 was performed for the two-group comparison. For multiple group comparisons, one-way
635 ANOVA followed by post-hoc Fisher's LSD test was used. Statistical significance was
636 predefined as $P<0.05$.

637

Authorship

L.B and S.R. contributed equally to the article. L.B., S.R and P.R conceived and designed the experiments. A.M., J.R. and H.K performed respiratory thermochemistry experiments. H.K. performed plethysmography and telemetry experiments. B.M., G.D., L.B. and H.K., performed AGS in DBA/2 mice. H.K. and B.G. performed histochemistry and RT-qPCR experiments. L.B., S.R., M.O. and H.K. analyzed data. L.B., S.R. and H.K. wrote the paper.

Acknowledgements

We thank for their assistance: Frédérique Cohen-Adad (scientific documentation; TIGER team, CRNL), and Denis Ressnikoff (confocal microscopy; Centre Commun de Quantimétrie of the Claude Bernard Lyon 1 University). Benoît Martin has received subventions from Eisai, UCB-Pharma and Zogenix.

Conflicts of interest

None of the authors has any conflict of interest to disclose. We confirm that we have read the Journal's position on issues involved in ethical publication and affirm that this report is consistent with those guidelines.

References

1. Lacuey, N., et al., The incidence and significance of periictal apnea in epileptic seizures. Epilepsia, 2018. **59**(3): p. 573-582.
2. Bourdillon, P., et al., Letter to the Editor. Temporal lobe epilepsy: open or stereotactic surgery? J Neurosurg, 2019. **131**(3): p. 989.
3. Ryvlin, P., et al., Incidence and mechanisms of cardiorespiratory arrests in epilepsy monitoring units (MORTEMUS): a retrospective study. Lancet Neurol, 2013. **12**(10): p. 966-77.

661 4. Vilella, L., et al., Incidence, Recurrence, and Risk Factors for Peri-ictal Central Apnea and
662 Sudden Unexpected Death in Epilepsy. Front Neurol, 2019. **10**: p. 166.
663 5. Sivathamboo, S., et al., Sleep-disordered breathing in epilepsy: epidemiology,
664 mechanisms, and treatment. Sleep, 2018. **41**(4).
665 6. Somboon, T., M.M. Grigg-Damberger, and N. Foldvary-Schaefer, Epilepsy and Sleep-
666 Related Breathing Disturbances. Chest, 2019. **156**(1): p. 172-181.
667 7. Patodia, S., et al., The ventrolateral medulla and medullary raphe in sudden unexpected
668 death in epilepsy. Brain, 2018. **141**(6): p. 1719-1733.
669 8. Garcia, A.J., 3rd, et al., Chapter 3--networks within networks: the neuronal control of
670 breathing. Prog Brain Res, 2011. **188**: p. 31-50.
671 9. Faingold, C.L., et al., Differences in serotonin receptor expression in the brainstem may
672 explain the differential ability of a serotonin agonist to block seizure-induced sudden
673 death in DBA/2 vs. DBA/1 mice. Brain Res, 2011. **1418**: p. 104-10.
674 10. Uteshev, V.V., et al., Abnormal serotonin receptor expression in DBA/2 mice associated
675 with susceptibility to sudden death due to respiratory arrest. Epilepsy Res, 2010. **88**(2-
676 3): p. 183-8.
677 11. Martin, B., et al., Audiogenic seizure as a model of sudden death in epilepsy: A
678 comparative study between four inbred mouse strains from early life to adulthood.
679 Epilepsia, 2020.
680 12. Faingold, C.L., S. Tupal, and M. Randall, Prevention of seizure-induced sudden death in a
681 chronic SUDEP model by semichronic administration of a selective serotonin reuptake
682 inhibitor. Epilepsy Behav, 2011. **22**(2): p. 186-90.
683 13. Tupal, S. and C.L. Faingold, Evidence supporting a role of serotonin in modulation of
684 sudden death induced by seizures in DBA/2 mice. Epilepsia, 2006. **47**(1): p. 21-6.
685 14. Curia, G., et al., The pilocarpine model of temporal lobe epilepsy. J Neurosci Methods,
686 2008. **172**(2): p. 143-57.
687 15. Biagini, G., et al., Proepileptic influence of a focal vascular lesion affecting entorhinal
688 cortex-CA3 connections after status epilepticus. J Neuropathol Exp Neurol, 2008. **67**(7):
689 p. 687-701.
690 16. Feher, J.J., Quantitative human physiology : an introduction. Second edition. ed.
691 Academic Press series in biomedical engineering. 2017, Amsterdam ; Boston:
692 Elsevier/AP, Academic Press is an imprint of Elsevier. xiii, 968 pages.

17. Venit, E.L., B.D. Shepard, and T.N. Seyfried, Oxygenation prevents sudden death in seizure-prone mice. Epilepsia, 2004. **45**(8): p. 993-6.
18. Aiba, I. and J.L. Noebels, Spreading depolarization in the brainstem mediates sudden cardiorespiratory arrest in mouse SUDEP models. Sci Transl Med, 2015. **7**(282): p. 282ra46.
19. Jefferys, J.G.R., et al., Brainstem activity, apnea, and death during seizures induced by intrahippocampal kainic acid in anaesthetized rats. Epilepsia, 2019. **60**(12): p. 2346-2358.
20. Faingold, C.L., M. Randall, and S. Tupal, DBA/1 mice exhibit chronic susceptibility to audiogenic seizures followed by sudden death associated with respiratory arrest. Epilepsy Behav, 2010. **17**(4): p. 436-40.
21. Johnston, S.C., et al., Central apnea and acute cardiac ischemia in a sheep model of epileptic sudden death. Ann Neurol, 1997. **42**(4): p. 588-94.
22. Kim, Y., et al., Severe peri-ictal respiratory dysfunction is common in Dravet syndrome. J Clin Invest, 2018. **128**(3): p. 1141-1153.
23. Lertwittayanon, W., O. Devinsky, and P.L. Carlen, Cardiorespiratory depression from brainstem seizure activity in freely moving rats. Neurobiol Dis, 2019. **134**: p. 104628.
24. Nakase, K., et al., Laryngospasm, central and obstructive apnea during seizures: Defining pathophysiology for sudden death in a rat model. Epilepsy Res, 2016. **128**: p. 126-139.
25. St-John, W.M., et al., Changes in respiratory-modulated neural activities, consistent with obstructive and central apnea, during fictive seizures in an in situ anaesthetized rat preparation. Epilepsy Res, 2006. **70**(2-3): p. 218-28.
26. Totola, L.T., et al., Impaired central respiratory chemoreflex in an experimental genetic model of epilepsy. J Physiol, 2017. **595**(3): p. 983-999.
27. Villiere, S.M., et al., Seizure-associated central apnea in a rat model: Evidence for resetting the respiratory rhythm and activation of the diving reflex. Neurobiol Dis, 2017. **101**: p. 8-15.
28. Sanchez, P.E., et al., Optimal neuroprotection by erythropoietin requires elevated expression of its receptor in neurons. Proc Natl Acad Sci U S A, 2009. **106**(24): p. 9848-53.
29. Maia, O.A.C., et al., Pilocarpine-induced status epilepticus reduces chemosensory control of breathing. Brain Res Bull, 2020. **161**: p. 98-105.
30. Kudin, A.P., et al., Seizure-dependent modulation of mitochondrial oxidative phosphorylation in rat hippocampus. Eur J Neurosci, 2002. **15**(7): p. 1105-14.

725 31. Kunz, W.S., et al., Mitochondrial complex I deficiency in the epileptic focus of patients
726 with temporal lobe epilepsy. Ann Neurol, 2000. **48**(5): p. 766-73.
727 32. Gastinger, S., et al., A comparison between ventilation and heart rate as indicator of
728 oxygen uptake during different intensities of exercise. J Sports Sci Med, 2010. **9**(1): p.
729 110-8.
730 33. Gautier, H., Interactions among metabolic rate, hypoxia, and control of breathing. J Appl
731 Physiol (1985), 1996. **81**(2): p. 521-7.
732 34. Refinetti, R., Metabolic heat production, heat loss and the circadian rhythm of body
733 temperature in the rat. Exp Physiol, 2003. **88**(3): p. 423-9.
734 35. Refinetti, R., The circadian rhythm of body temperature. Front Biosci (Landmark Ed),
735 2010. **15**: p. 564-94.
736 36. Seifert, E.L. and J.P. Mortola, Circadian pattern of ventilation during acute and chronic
737 hypercapnia in conscious adult rats. Am J Physiol Regul Integr Comp Physiol, 2002.
738 **282**(1): p. R244-51.
739 37. Stephenson, R., et al., Circadian rhythms and sleep have additive effects on respiration
740 in the rat. J Physiol, 2001. **536**(Pt 1): p. 225-35.
741 38. Pearce, P.S., et al., Metabolic injury in a variable rat model of post-status epilepticus.
742 Epilepsia, 2016. **57**(12): p. 1978-1986.
743 39. Luks, A., R.W. Glenny, and H.T. Robertson, Introduction to cardiopulmonary exercise
744 testing. 2013, New York: Springer. vii, 147 pages.
745 40. Poets, C.F., et al., Gasping and other cardiorespiratory patterns during sudden infant
746 deaths. Pediatr Res, 1999. **45**(3): p. 350-4.
747 41. Campos, R.R., F.R. Tolentino-Silva, and L.E. Mello, Respiratory pattern in a rat model of
748 epilepsy. Epilepsia, 2003. **44**(5): p. 712-7.
749 42. Totola, L.T., et al., Amygdala rapid kindling impairs breathing in response to chemoreflex
750 activation. Brain Res, 2019. **1718**: p. 159-168.
751 43. Hodges, M.R. and G.B. Richerson, Interaction between defects in ventilatory and
752 thermoregulatory control in mice lacking 5-HT neurons. Respir Physiol Neurobiol, 2008.
753 **164**(3): p. 350-7.
754 44. Morales, A., et al., Unexpected expression of orexin-B in basal conditions and increased
755 levels in the adult rat hippocampus during pilocarpine-induced epileptogenesis. Brain
756 Res, 2006. **1109**(1): p. 164-75.

757 45. Nadam, J., et al., Neuroprotective effects of erythropoietin in the rat hippocampus after
758 pilocarpine-induced status epilepticus. Neurobiol Dis, 2007. **25**(2): p. 412-26.
759 46. Navarro, F.P., et al., Brain heparanase expression is up-regulated during postnatal
760 development and hypoxia-induced neovascularization in adult rats. J Neurochem, 2008.
761 **105**(1): p. 34-45.
762 47. Manouze, H., et al., Effects of Single Cage Housing on Stress, Cognitive, and Seizure
763 Parameters in the Rat and Mouse Pilocarpine Models of Epilepsy. eNeuro, 2019. **6**(4).
764 48. Dube, C., et al., Relationship between neuronal loss and interictal glucose metabolism
765 during the chronic phase of the lithium-pilocarpine model of epilepsy in the immature
766 and adult rat. Exp Neurol, 2001. **167**(2): p. 227-41.
767 49. Leroy, C., et al., Temporal changes in mRNA expression of the brain nutrient
768 transporters in the lithium-pilocarpine model of epilepsy in the immature and adult rat.
769 Neurobiol Dis, 2011. **43**(3): p. 588-97.
770 50. Racine, R.J., Modification of seizure activity by electrical stimulation. II. Motor seizure.
771 Electroencephalogr Clin Neurophysiol, 1972. **32**(3): p. 281-94.
772 51. Belouze, M., et al., Leanness of Lou/C rats does not require higher thermogenic capacity
773 of brown adipose tissue. Physiol Behav, 2011. **104**(5): p. 893-9.
774 52. Ogier, M., et al., Brain-derived neurotrophic factor expression and respiratory function
775 improve after ampakine treatment in a mouse model of Rett syndrome. J Neurosci,
776 2007. **27**(40): p. 10912-7.
777

778

779 ## Figure legends

780 **Figure 1: Detection of SDOC events during a 24-hour monitoring of oxygen consumption in**
781 **a subgroup of epileptic rats.** Oxygen consumption ($\dot{V}O_2$) (light period from 06:00 am to 6:00
782 pm) was measured using respiratory thermochemistry. Grey bar above each x-axis indicates
783 the dark period. A single profile was observed in control rats (A), while two distinct profiles
784 were distinguished in epileptic rats (B, C). The first profile was similar to that observed in
785 control rats (B), the second one was characterized by several episodes of sharp decrease in
786 oxygen consumption (SDOC) (C), sometimes reaching the zero value. These SDOC events
787 were only seen in epileptic rats, thereby discriminating two groups of epileptic rats upon
788 their presence (EPI/SDOC+) or their absence (EPI/SDOC-).

789 **Figure 2: SDOC can occur independently of behavioral spontaneous seizures.** (A) Example
790 of a SDOC event recorded in an EPI rat at 5 weeks post-SE, when it was adopting a sleep
791 posture. This SDOC event occurred during the light period and was identified with the
792 decline in $\dot{V}O_2$ values. No behavioral seizure was observed before, during and after the SDOC
793 occurrence. By contrast, (B) a sharp increase in $\dot{V}O_2$ values was observed after a 43-second
794 stage-5 seizure according to Racine's scale in an EPI/SDOC+ rat whose values of $\dot{V}O_2$ were
795 above pre-ictal level for about 30 minutes.

796 **Figure 3: Time course of daily $\dot{V}O_2$ pattern. Respiratory thermochemistry was recorded**
797 **once a week for each rat, from the 1st to the 8th week post-SE.** (A) Daily $\dot{V}O_2$ is calculated for
798 each group (control rats (n=8), EPI/SDOC- rats (n=14), EPI/SDOC+ rats (n=6)) from the 1 to 8
799 weeks post-SE. (B) The daily $\dot{V}O_2$ of animals is calculated at 3-4 weeks post-SE in animals
800 identified or not yet as EPI/SDOC+ rats. Paired comparison of daily $\dot{V}O_2$ over weeks showed
801 statistical significance with only 1-2 weeks post-SE. Results are expressed in mean ± SEM of

802 $\dot{V}O2$, *, p<0.05; **, P=0.01 in comparison of daily $\dot{V}O_2$ at 1-2 weeks post-SE. (C) the first
803 SDOC was detected in one rat (1/20) during the 3rd post-SE week. The maximum number of
804 EPI rats exhibiting SDOCs (EPI/SDOC+, 30%) was reached by the end of the 5th week post-SE.
805 The proportion of EPI/SDOC+ rats was expressed in percent of the total number of rats
806 developing epilepsy (yellow curve) or in percent of the total number of rats presenting with
807 SDOCs by the end of the 8th post-SE (red curve).

808 **Figure 4: Semi-quantification of 5-HT immunopositive terminals of caudal raphe nuclei**
809 **within the medulla oblongata of control and EPI rats.** Fluorescent 5-HT labeling was
810 performed on sections selected at interaural -2.60 mm within two brainstem regions
811 involved in the regulation of respiratory rhythm generation: the ventrolateral medulla (VLM)
812 and nucleus tractus solitarius (NTS). Images of 5-HT positive fibers were captured within the
813 VLM (A1, A2, A3) and the NTS (B1, B2, B3) using confocal microscopy (x63 objective). Density
814 of 5-HT positive fibers was calculated in the VLM (A4) and the NTS (B4). Data are expressed
815 as the mean ± SEM (n=3 per group). *, P<0.05; ***, P<0.001, compared to controls and †††,
816 P<0.001, compared to EPI/SDOC-.

817 **Figure 5: TPH2 and SERT mRNA transcript levels were measured in the brainstem of EPI**
818 **rats and DBA/2 mice.** Changes in brainstem levels of TPH2 (A) and SERT (B) transcripts were
819 measured in EPI rats and DBA/2 mice at 8 weeks post-SE and 2-3 minutes after an
820 audiogenic seizure (AGS), respectively. In contrast to EPI rats, DBA/2 mice had no history of
821 seizure before AGS. Some mice developed a fatal respiratory arrest (DBA/2 with FRA) or a
822 non-fatal respiratory arrest (DBA/2 with NFRA) after an AGS. TPH2 and SERT transcript levels
823 in EPI/SDOC+ rats and in DBA/2 with FRA mice are expressed in percentage (mean ± SEM) of
824 EPI/SDOC- rats and DBA/2 mice with NFRA, respectively (n=5 in each group). †: P<0.05, ††:

825 P<0.01, †††: P<0.001, in comparison to EPI/SDOC- group for rat and DBA/2 with FRA group
826 for mice. *, P<0.05; **, P<0.01, in comparison to control rats.
827

828 ## Table legend

829 **Table 1: Monitoring of cardio-respiratory functions in control and EPI rats between 12 and**
830 **15 weeks post-SE.** Using plethysmography, the ventilatory variables were measured under
831 normoxic condition (21% O_2) at 12 weeks post-SE (A) and in response to hypoxia (9% O_2) or
832 hypercapnia (5% CO_2) exposures between 13-14 weeks post-SE (B). Cardiac frequency (C)
833 and body-temperature (D) were concomitantly evaluated at 15 weeks post-SE.
834 Abbreviations: Fc, cardiac frequency; f_R, respiratory frequency; T_B, body-temperature; T_E,
835 expiration time; T_I, inspiration time; T_{tot}, total respiratory cycle duration; $\dot{V}_E$, minute volume;
836 V_T, tidal volume. Statistics: NT, not statistically significant.
837

838 ## Supplementary information

839 **Figure S1: Metabolic rate of oxygen at 1-2 weeks and 5-8 weeks post-SE.** The average
840 oxygen consumption ($\dot{V}$O2) was calculated for the light and dark periods at 5-8 weeks post-
841 SE (A) and then at 1-2 weeks post-SE (B) using the same experimental groups,
842 retrospectively. Dichotomization of SDOC+ and SDOC- EPI rats was based on data collected
843 at 5-8 weeks post-SE, which showed a significant decline in the average $\dot{V}$O2 of EPI/SDOC+
844 rats during both the light and dark periods compared to EPI/SDOC- and control rats (A).
845 There was no difference the three rat groups at 1-2 weeks post-SE, during which time no
846 SDOCs were detected (B). Results are expressed in percent of control rats *, P<0.05; ***,
847 p<0.001, compared to control rats. †††, P<0.001, compared to EPI/SDOC- rats.

848

849 **Figure S2: Ventilatory function in epileptic and control rats under normoxia**. (A) ventilation
850 (V_E), respiratory frequency (F_R) and tidal volume (V_T) of epileptic (n=16) and control (n=5)
851 rats at 12 weeks post-*SE.* (B) Index of pattern stability includes coefficient of variation of
852 ventilatory pattern and apnea number/duration. The results are expressed as the mean ±
853 SEM. *, P<0.05; **, P<0.01, in comparison to control rats.

854

855 **Supplementary Table S1: Primer pairs used for qPCR amplification of TPH2 and SERT**
856 **cDNAs of rat and mouse.**

857

858 ## Key Points

859 • There are mild and severe patterns of respiratory dysfunctions among rats with epilepsy
860 developed after pilocarpine induced *status epilepticus*.
861 • Severe respiratory dysfunctions were evidenced in 30-50% of rats with epilepsy.
862 • These dysfunctions consisted with intermittent episodes of sharp decrease in oxygen
863 consumption (SDOC), slow breathing pattern and low metabolic rate of oxygen at rest.
864 • SDOCs were associated with decreased density of 5-HT-containing processes in the
865 nucleus tractus solitarius.
866 • Rats with SDOCs had SERT and TPH2 transcript level alterations similar to DBA/2 mice
867 subjected to AGS-induced fatal respiratory arrest.

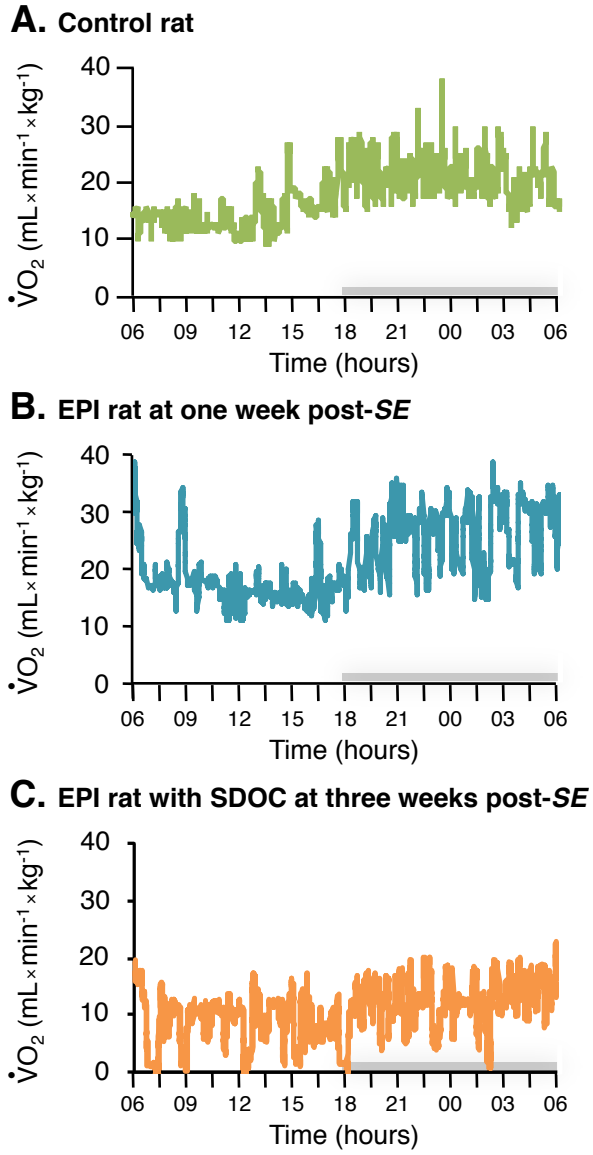

Figure 1: Detection of SDOC events during a 24-hour monitoring of oxygen consumption in a subgroup of epileptic rats. Oxygen consumption ($\dot{V}O_2$) (light period from 06:00 am to 6:00 pm) was measured using respiratory thermochemistry. Grey bar above each x-axis indicates the dark period. A single profile was observed in control rats (A), while two distinct profiles were distinguished in epileptic rats (B, C). The first profile was similar to that observed in control rats (B), the second one was characterized by several episodes of sharp decrease in oxygen consumption (SDOC) (C), sometimes reaching the zero value. These SDOC events were only seen in epileptic rats, thereby discriminating two groups of epileptic rats upon their presence (EPI/SDOC+) or their absence (EPI/SDOC-).

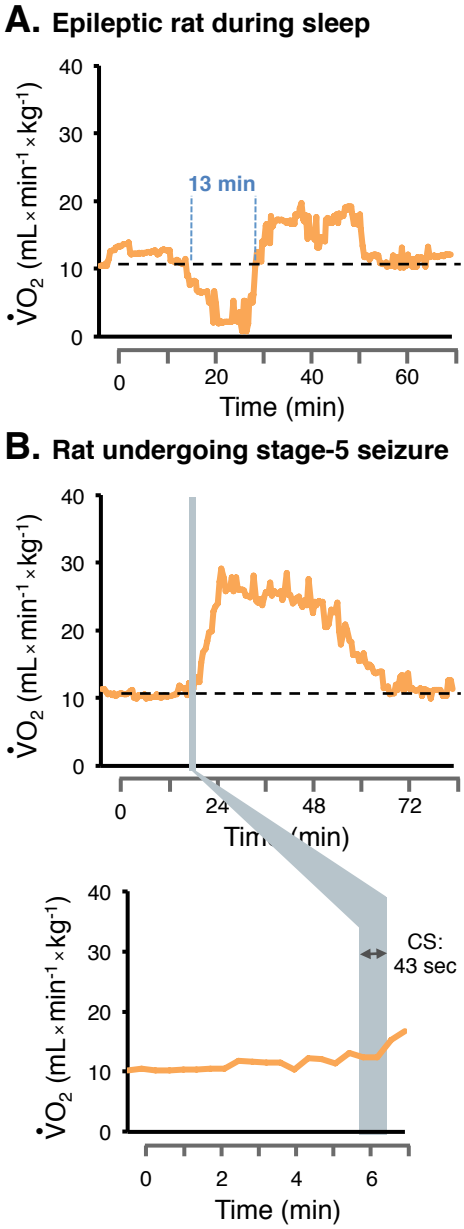

Figure 2: SDOC can occur independently of behavioral spontaneous seizures. (A) Example of a SDOC event recorded in an EPI rat at 5 weeks post-SE, when it was adopting a sleep posture. This SDOC event occurred during the light period and was identified with the decline in $\dot{V}O_2$ values. No behavioral seizure was observed before, during and after the SDOC occurrence. By contrast, (B) a sharp increase in $\dot{V}O_2$ values was observed after a 43-second stage-5 seizure according to Racine's scale in an EPI/SDOC+ rat whose values of $\dot{V}O_2$ were above pre-ictal level for about 30 minutes.

A. Time course of the daily $\dot{V}O2$ in experimental groups

	Daily $\dot{V}O2$ (mL x min^{-1} x kg^{-1})		
Weeks post-SE	Control rats (n=8)	EPI/SDOC- rats (n=14)	EPI/SDOC+ rats (n=6)
8	19.2 ± 0.6 *	18.0 ± 0.5 *	8.1 ± 0.3 **
7	18.1 ± 0.4 *	19.8 ± 0.5	10.1 ± 1.6 *
6	20.0 ± 0.4	19.9 ± 0.8	11.0 ± 2.5 *p=0.09*
5	19.8 ± 0.1	22.3 ± 1.2	12.5 ± 1.6 *
4	20.8 ± 0.5	20.1 ± 0.6	
3	21.2 ± 0.9	21.0 ± 0.8	
1-2	24.4 ± 1.1	23.1 ± 1.7	26.6 ± 1.0

B. Time course of the daily $\dot{V}O2$ in EPI/SDOC+ rats

	Rats identified as EPI/SDOC+		Rats not yet identified as EPI/SDOC+	
Weeks post-SE	n	Daily $\dot{V}O2$ (mL x min^{-1} x kg^{-1})	n	Daily $\dot{V}O2$ (mL x min^{-1} x kg^{-1})
4	3/6	13.5 ± 3.5	3/6	20.1 ± 1.8
3	1/6	17.2	5/6	21.1 ± 1.9

C. Time course of SDOC appearance by EPI rats

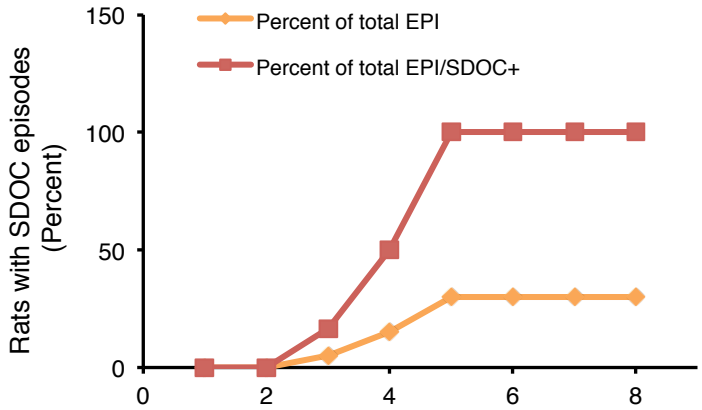

Figure 3: Time course of daily $\dot{V}O_2$ pattern. Respiratory thermochemistry was recorded once a week for each rat, from the 1st to the 8th week post-SE. (A) Daily $\dot{V}O_2$ is calculated for each group (control rats (n=8), EPI/SDOC- rats (n=14), EPI/SDOC+ rats (n=6)) from the 1 to 8 weeks post-SE. (B) The daily $\dot{V}O_2$ of animals is calculated at 3-4 weeks post-SE in animals identified or not yet as EPI/SDOC+ rats. Paired comparison of daily $\dot{V}O_2$ over weeks showed statistical significance with only 1-2 weeks post-SE. Results are expressed in mean ± SEM of $\dot{V}O2$, *, $p<0.05$; **, $p=0.01$ in comparison of daily $\dot{V}O_2$ at 1-2 weeks post-SE. (C) the first SDOC was detected in one rat (1/20) during the 3rd post-SE week. The maximum number of EPI rats exhibiting SDOCs (EPI/SDOC+, 30%) was reached by the end of the 5th week post-SE. The proportion of EPI/SDOC+ rats was expressed in percent of the total number of rats developing epilepsy (yellow curve) or in percent of the total number of rats presenting with SDOCs by the end of the 8th post-SE (red curve).

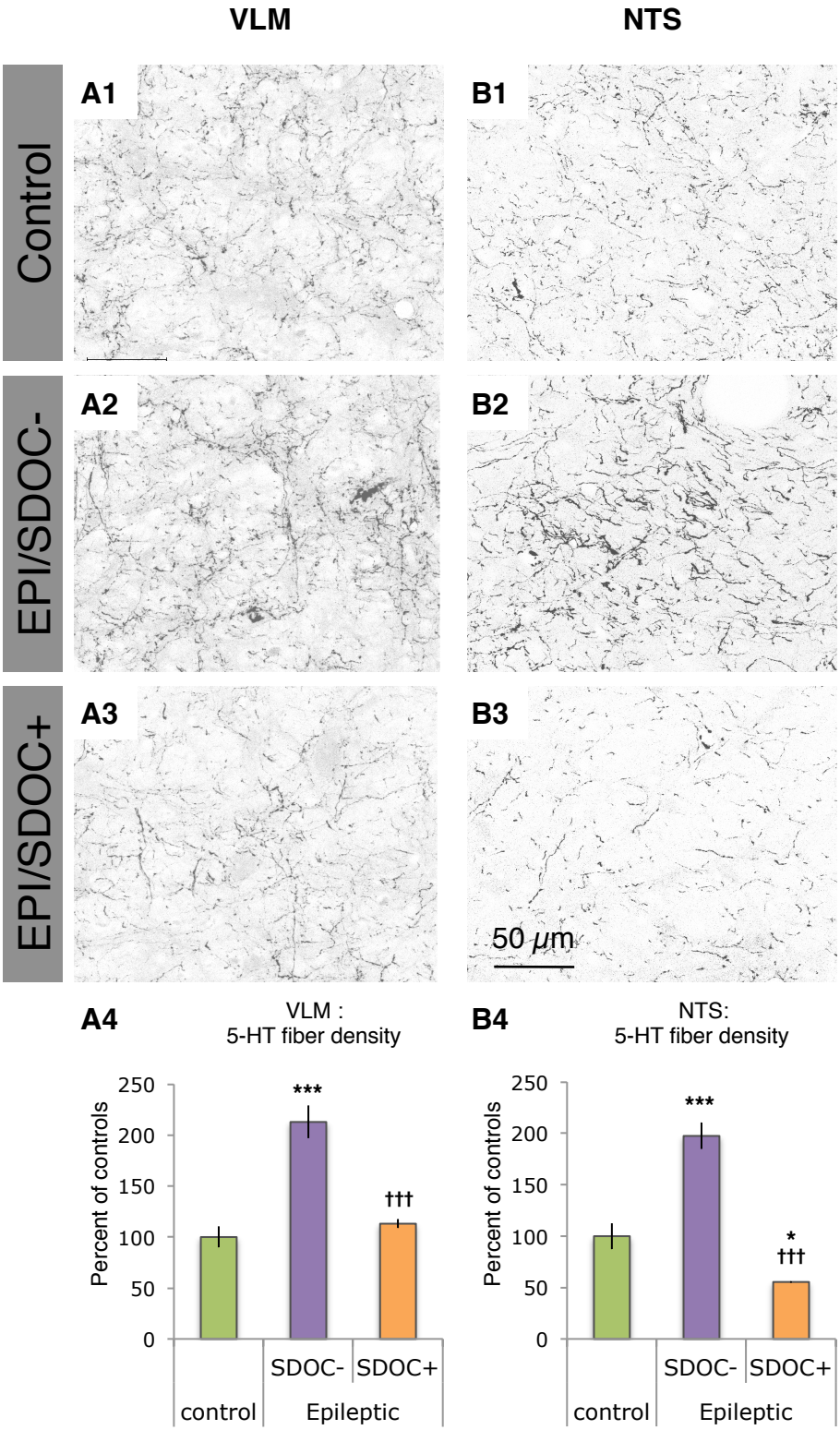

Figure 4: Semi-quantification of 5-HT immunopositive terminals of caudal raphe nuclei within the medulla oblongata of control and EPI rats. Fluorescent 5-HT labeling was performed on sections selected at interaural -2.60 mm within two brainstem regions involved in the regulation of respiratory rhythm generation: the ventrolateral medulla (VLM) and nucleus tractus solitarius (NTS). Images of 5-HT positive fibers were captured within the VLM (A1, A2, A3) and the NTS (B1, B2, B3) using confocal microscopy (x63 objective). Density of 5-HT positive fibers was calculated in the VLM (A4) and the NTS (B4). Data are expressed as the mean ± SEM (n=3 per group). *, $p<0.05$; ***, $p<0.001$, compared to controls and †††, $p<0.001$, compared to EPI/SDOC-.

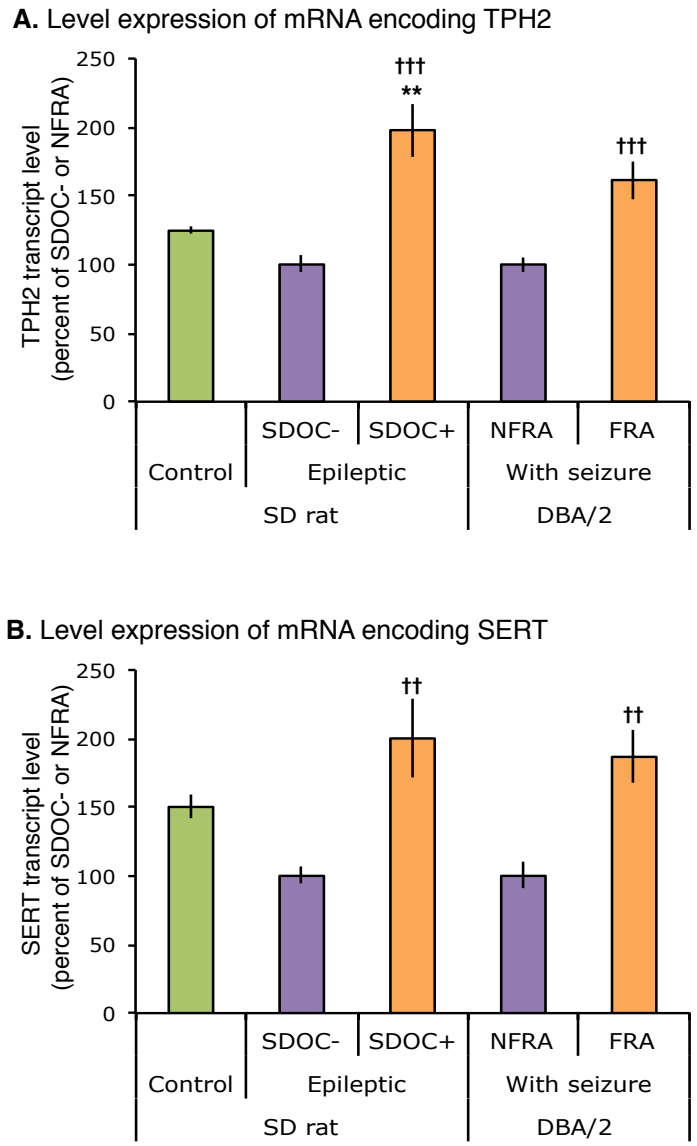

Figure 5: TPH2 and SERT mRNA transcript levels were measured in the brainstem of EPI rats and DBA/2 mice. Changes in brainstem levels of TPH2 (A) and SERT (B) transcripts were measured in EPI rats and DBA/2 mice at 8 weeks post-SE and 2-3 minutes after an audiogenic seizure (AGS), respectively. In contrast to EPI rats, DBA/2 mice had no history of seizure before AGS. Some mice developed a fatal respiratory arrest (DBA/2 with FRA) or a non-fatal respiratory arrest (DBA/2 with NFRA) after an AGS. TPH2 and SERT transcript levels in EPI/SDOC+ rats and in DBA/2 with FRA mice are expressed in percentage (mean ± SEM) of EPI/SDOC- rats and DBA/2 mice with NFRA, respectively (n=5 in each group). †: $p<0.05$, ††: $p<0.01$, †††: $p<0.001$, in comparison to EPI/SDOC- group for rat and DBA/2 with FRA group for mice. *, $p<0.05$; **, $p<0.01$, in comparison to control rats.

A- Basal respiratory variables under normoxia at 12 weeks post-*SE*

	Control (n=5)	EPI/SDOC- (n=8)	EPI/SDOC+ (n=8)	Ctrl vs SDOC- (P value)	Ctrl vs SDOC + (P value)	SDOC+ vs SDOC- (P value)
$\dot{V}_E$ (mL×min^{-1}×100g^{-1})	32 ± 1	30 ± 1	26 ± 1	*0.274*	0.002	0.013
f_R (breath×min^{-1})	101 ± 3	93 ± 2	87 ± 2	0.015	<0.001	0.036
V_T (mL×100g^{-1})	0.32 ± 0.01	0.33 ± 0.01	0.31 ± 0.01	*NT*	*NT*	*NT*
T_I (msec)	207 ± 7	233 ± 3	263 ± 8	0.015	<0.001	<0.001
T_E (msec)	385 ± 12	413 ± 9	438 ± 10	*0.088*	0.003	*0.083*
T_{tot} (msec)	593 ± 14	646 ± 11	700 ± 17	0.025	<0.001	0.013
Apnea frequency x min^{-1}	0.32 ± 0.17	0.27 ± 0.13	0.10 ± 0.07	*NT*	*NT*	*NT*
Apnea duration (msec)	1339 ± 67	1435 ± 65	1477 ± 75	*NT*	*NT*	*NT*
Coefficient of variation	0.49 ± 0.01	0.53 ± 0.01	0.52 ± 0.02	*NT*	*NT*	*NT*

B- Respiratory response to hypoxia and hypercapnia at 13-14 weeks post-*SE*

% of baseline		Control (n=13)	EPI/SDOC- (n=12)	EPI/SDOC+ (n=6)	Ctrl vs SDOC- (P value)	Ctrl vs SDOC+ (P value)	SDOC+ *vs* SDOC- (P value)
Hypoxia *9% of O_2*	$\dot{V}_E$ (mL×min^{-1}×100g^{-1})	225 ± 9	273 ± 18	278 ± 19	0.019	0.046	*0.847*
	f_R (breath×min^{-1})	146 ± 5	171 ± 4	165 ± 3	<0.001	0.024	*0.463*
	V_T (mL×100g^{-1})	153 ± 5	169 ± 8	170 ± 7	*NT*	*NT*	*NT*
Hypercapnia *5% of CO_2*	$\dot{V}_E$ (mL×min^{-1}×100g^{-1})	187 ± 6	211± 8	219 ± 14	0.028	0.023	*0.562*
	f_R (breath×min^{-1})	128 ± 4	141 ± 4	141 ± 8	*NT*	*NT*	*NT*
	V_T (mL×100g^{-1})	141± 3	148 ± 5	153 ± 6	*NT*	*NT*	*NT*

C- Cardiac frequency at 15 weeks post-*SE*

		Control (n=3)	EPI/SDOC- (n=3)	EPI/SDOC+ (n=2)	Ctrl vs SDOC- (P value)	Ctrl vs SDOC+ (P value)	SDOC+ vs SDOC- (P value)
Day	F_C (beats×min^{-1})	315 ± 17	338 ± 11	333 ± 8	*NT*	*NT*	*NT*
Night	F_C (beats×min^{-1})	332 ± 19	355 ± 9	351 ± 12	*NT*	*NT*	*NT*

D- Body-temperature at 15 weeks post-*SE*

		Control (n=3)	EPI/SDOC- (n=3)	EPI/SDOC+ (n=2)	Ctrl vs SDOC- (P value)	Ctrl vs SDOC+ (P value)	SDOC+ vs SDOC- (P value)
Day	T_B (degree C°)	37.5 ± 0.1	37.6 ± 0.1	37.7 ± 0.2	*NT*	*NT*	*NT*
Night	T_B (degree C°)	38 ± 0.2	37.9 ± 0.1	38.1 ± 0.1	*NT*	*NT*	*NT*

Table 1: Monitoring of cardio-respiratory functions in control and EPI rats between 12 and 15 weeks post-SE. Using plethysmography, the ventilatory variables were measured under normoxic condition (21% O_2) at 12 weeks post-SE (A) and in response to hypoxia (9% O_2) or hypercapnia (5% CO_2) exposures between 13-14 weeks post-SE (B). Cardiac frequency (C) and body-temperature (D) were concomitantly evaluated at 15 weeks post-SE. Abbreviations: Fc, cardiac frequency; f_R, respiratory frequency; T_B, body-temperature; T_E, expiration time; T_I, inspiration time; T_{tot}, total respiratory cycle duration; $\dot{V}_E$, minute volume; V_T, tidal volume. Statistics: NT, not statistically significant.